Chapter 2

Experimental Techniques

This chapter describes the experimental procedures followed for studies of isotopic composition of solids using the secondary ion mass spectrometer or the ion microprobe. A brief description of the working principle of the Cameca Ims-4f ion microprobe used in this work is provided along with results obtained from parametric studies that confirm the suitability of the ion microprobe for high precision, high mass resolution isotopic studies. Basic principles used in data synthesis are discussed and results obtained from isotopic analyses of terrestrial standards and isotopically doped silicate glasses are also presented to illustrate the precision and reproducibility that may be obtained with our ion microprobe.

2.1 The Cameca Ims-4f Ion Microprobe

The Cameca Ims-4f ion microprobe is a double focussing mass spectrometer which also has the unique capability of ion imaging. It uses energetic (keV) primary ion beam to bombard the sample surface and generate secondary ions. The secondary ions are energized, energy filtered and mass analyzed and are detected using suitable ion counting system. A general schematic of the ion microprobe is shown in Fig. 2.1. The principles of secondary ion mass spectrometry have been reviewed by Benninghoven et al. (1987) and the details of optical design of the Cameca Ims-3f ion microprobe have been presented by Lapareur (1980).

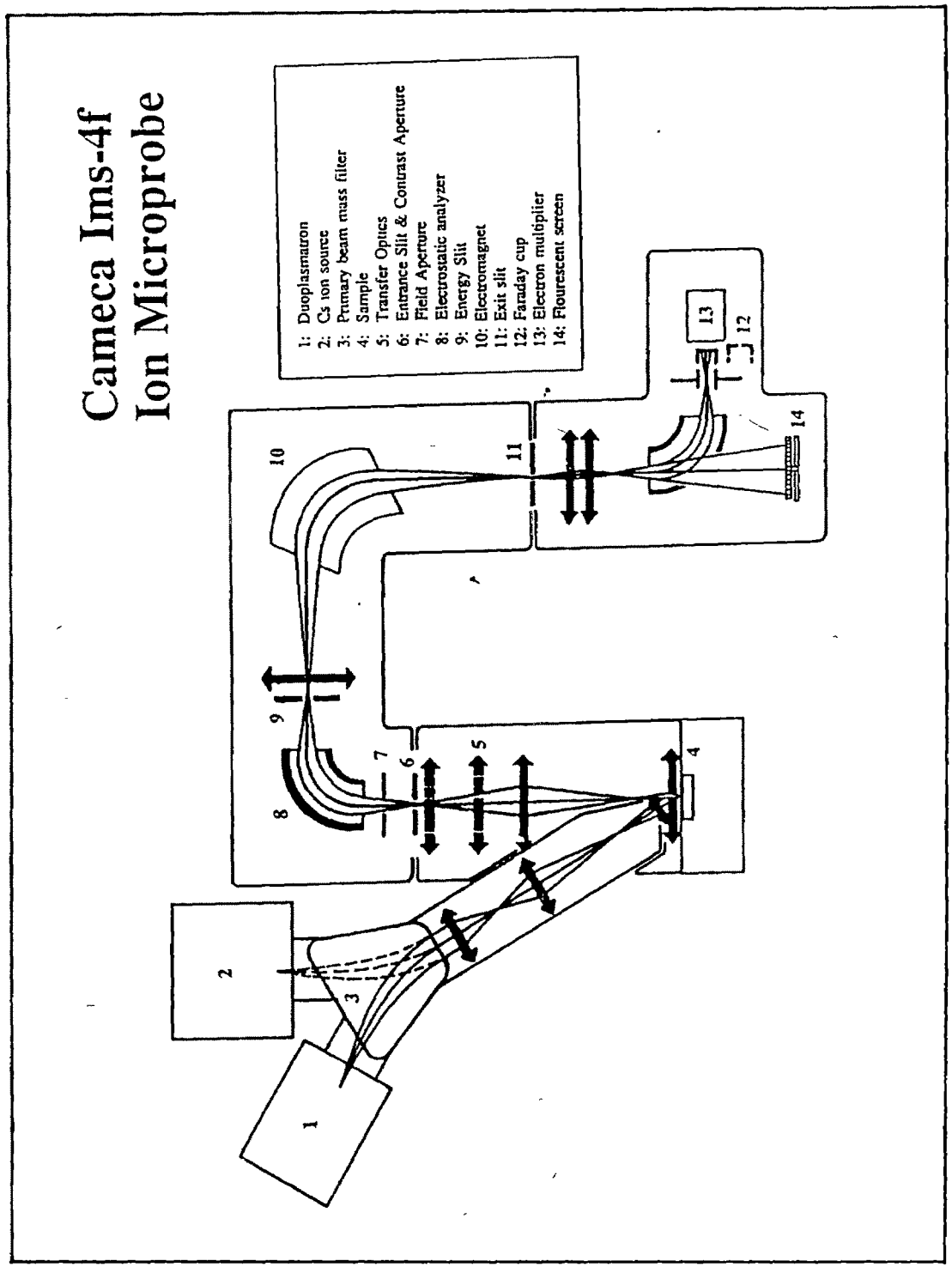

Figure 2.1: A schematic of the ion microprobe (Cameca Ims-4f). The important sub-systems are labelled and ideal traces of both primary and secondary ion optics are shown.

2.1.1 Primary Ion Column

The primary ion column consists of the primary beam source and is followed by a flight tube which consists of a set of lenses and apertures which can be used to control the size and strength of primary beam impinging on the sample surface (Fig. 2.2). There are two primary ion beam sources, a Duoplasmatron (DP) and a thermal ionization source (TI).

The Duoplasmatron can be used to generate both positive and negative ions of a variety of atomic and molecular species (e.g. O, Ar, Xe); we use oxygen to produce $^{16}O^-$ and O_2^+ beam. Ions are produced in a cold hollow Ni cathode by arc-discharge. Energetic positive or negative primary ions are extracted by floating the source at a higher/lower potential with respect to the grounded extraction lens.

A conical lens (CL) is used to focus the primary ions extracted from the source. A set of deflectors (D2) is used to align the beam along the central path of the magnetic prism. The magnetic prism, known as the primary beam mass filter (PBMF), is used to deflect the primary ions into the flight tube. It also helps to clean the primary beam of impurities (e.g. H_2O, N_2, and NO in the case of Duoplasmatron).

A set of electrostatic lenses and apertures placed after the magnetic prism are used to focus the beam onto the sample surface. An electrostatic lens (L2), after the primary magnet focusses the beam at the position of the mass selection aperture (MSA). Deflector plates (D1) beyond this aperture align the primary beam along the principle axis of lens L1 which follows lens L2. The lens L1 is used to change the diameter of the beam at the position of primary beam aperture (PBA) thus allowing one to adjust the primary beam current on the sample surface. A set of stigmators (S1) and beam position deflectors (BPD) are placed immediately after the primary beam aperture. The beam position deflector is used to position the beam on the sample surface or to divert it into the Faraday cup (FC) to measure the primary current. The stigmators are in general used to produce a circular beam spot on the sample surface. Finally the lens L3 is used to focus the beam on the sample surface.

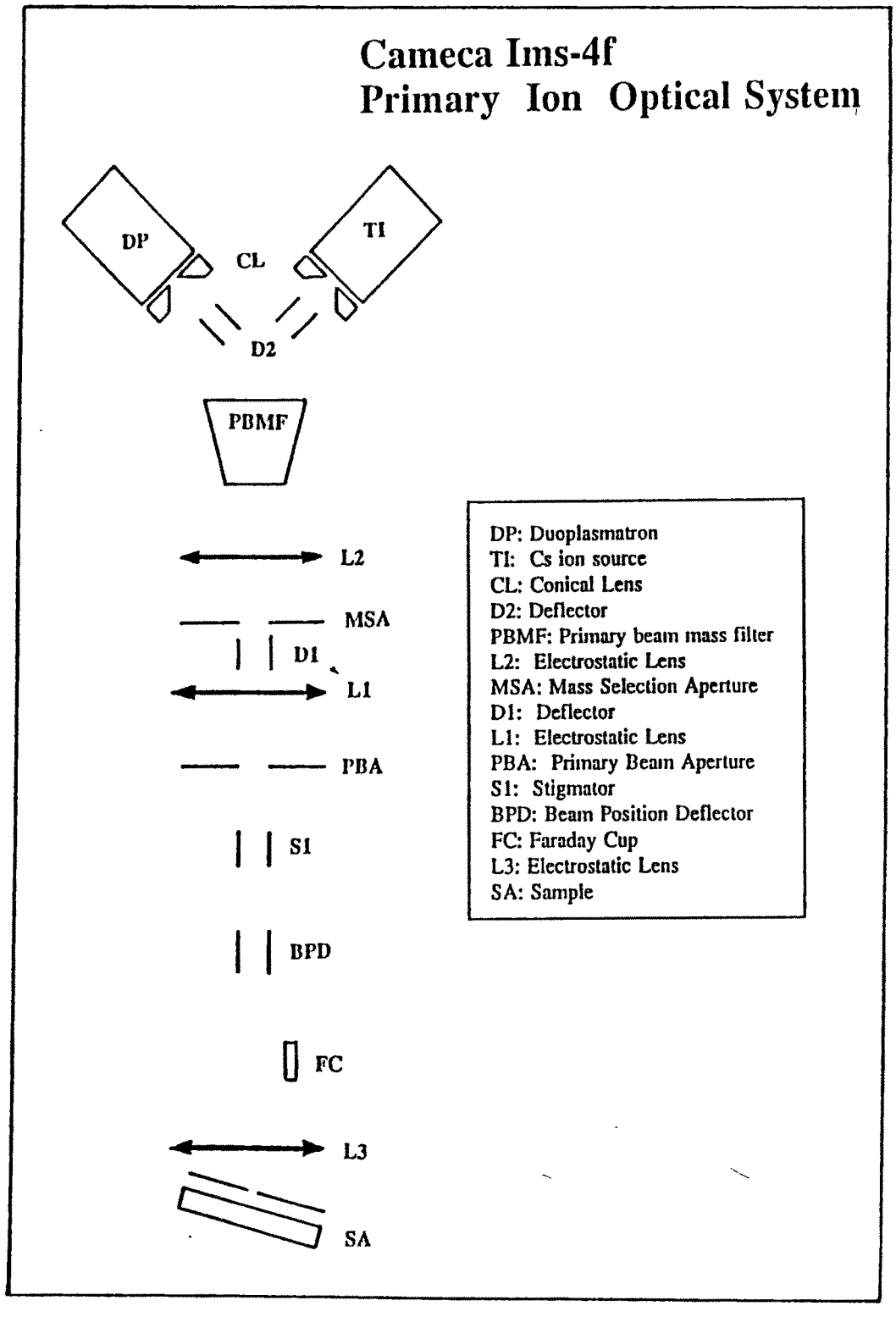

Figure 2.2: Schematic of the primary column of the ion microprobe. The important subsystems are labelled.

The choice of the primary beam and its polarity is made depending upon the elements to be analyzed. A combination of $^{16}O^-$ beam from the Duoplasmatron and positive secondary ions is used for analyzing elements like Mg, Al, K, Ca, Ti etc., while the combination of a Cs^+ beam from the thermal ionization source and negative secondary ions is used for analyzing electronegative elements like O, C, N, S etc.

In this study, isotopic analyses were carried out with a 17 keV $^{16}O^-$ focussed primary ion beam, with current in the nanoampere range. The corresponding size of the beam spot is generally $\leq 10\mu m$, that allowed the analysis of microphases. Studies of negative secondaries from insulating samples using Cs^+ beam is made difficult by the problem of sample charging and no attempt was made to study isotopic composition of elements (e.g. O) where this mode of operation is necessary. However, this problem can be overcome, in principle, by flooding the sample surface with low energy electron cloud (Slodzian et al. 1987).

2.1.2 Secondary Ion Column

The secondary ion column consists of the sample chamber, the transfer optics, the electrostatic and magnetic sectors, and a set of slits and apertures through which the secondary ions are transported and mass resolved. The mass resolved ions are detected using either a Faraday cup or pulse counting system. A schematic of the secondary ion optics is shown in Fig. 2.3.

The sample is kept at a potential of $\pm$4.5keV with respect to the grounded extraction plate (GP), the polarity depending on whether positive or negative secondary ions are chosen for analysis. The secondary ions are accelerated towards the grounded extraction plate that is placed 4.5mm away from the sample surface. The extraction plate that has a circular hole, also acts as the immersion lens of the transfer optics system which collimates the secondary ion beam towards the entrance slit of the mass spectrometer.

The immersion lens produces virtual images of the sample surface and the crossover

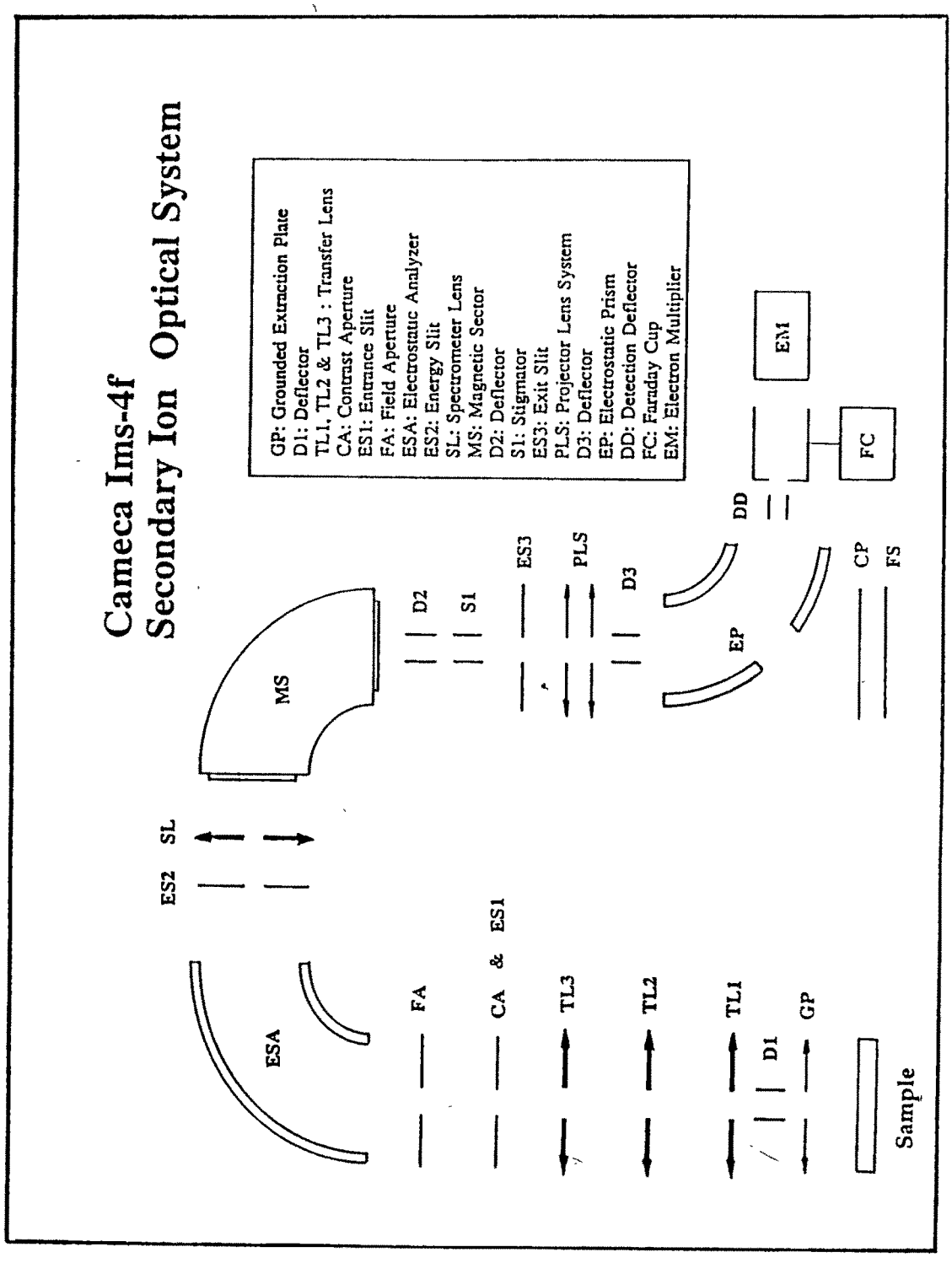

Figure 2.3: A schematic of the secondary ion column of the ion microprobe; the important subsystems are labelled.

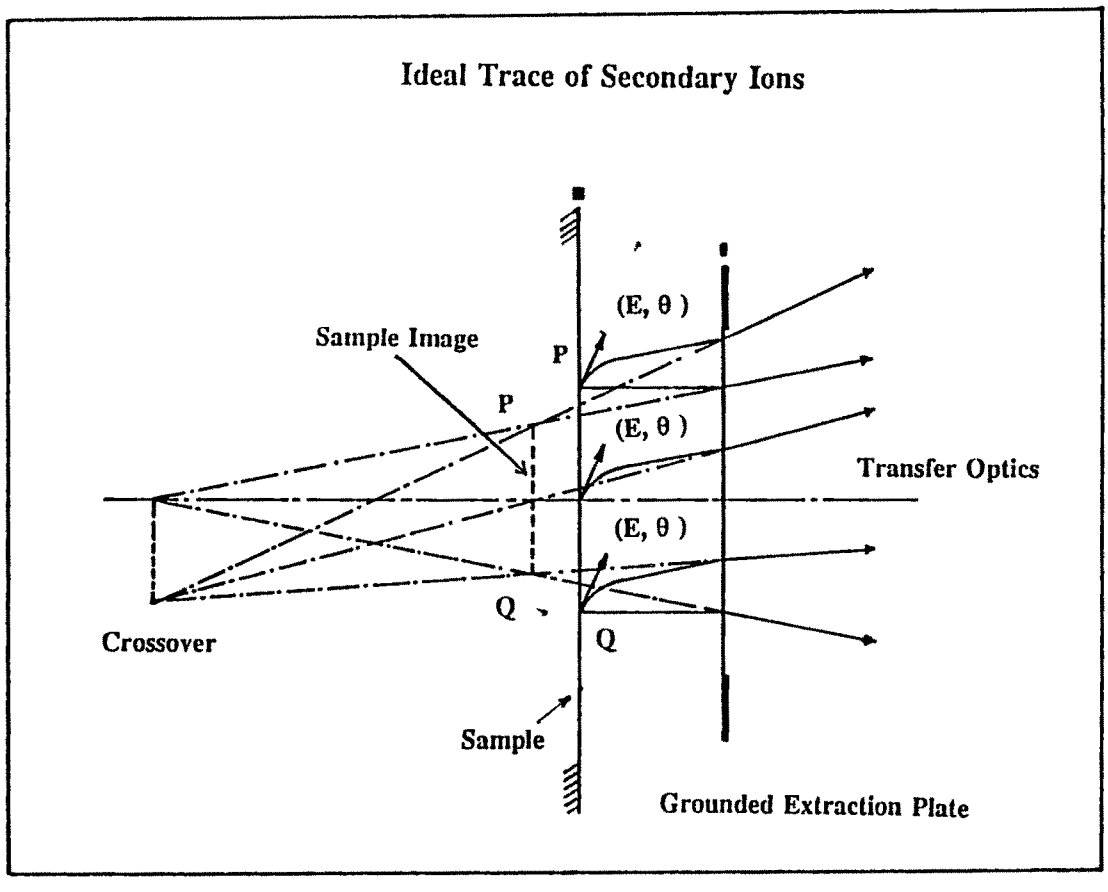

Figure 2.4: Ideal traces of the secondary ions from the sample surface are shown to illustrate the virtual image of the crossover or the illumination pupil.

(the illumination pupil) (Fig. 2.4). The size of the crossover is dependent on the lateral energy distribution of the secondary ions. A deflector (D1) placed after the immersion lens allows one to adjust the beam position with respect to the optic axis. The three lenses (TL1, TL2 and TL3) that follow the deflector are used to produce real image of the sample surface and the crossover in the plane of field aperture (FA) and contrast aperture (CA) respectively. These apertures are used to restrict the size of the crossover and the field of view as seen by the rest of the mass spectrometer. The ion microprobe transfer optics system can be used to provide preset imaged fields of 25μm, 150μm and 200μm. The 150μm imaged field is generally used for high mass resolution isotopic analyses [mass resolving power (MRP) (M/ΔM): 3000-10000]. Use of suitable field aperture allows one to restrict the sampling of ions from as small an area as 10μm of the sample surface.

The contrast aperture is used to restrict the size of the crossover thereby allowing only those ions with lateral energy below a certain value to enter the electrostatic analyzer (ESA). This not only reduces spherical aberrations but also improves the spatial resolution of the image. Additionally, the entrance slit (ES1) to the mass spectrometer system is also placed nearly coincident with the contrast aperture. The field aperture placed after the contrast aperture is coincident with the focal plane of the ESA and is used to restrict the transmission of ions only from a selected area.

The secondary ions sputtered from the sample surface have an energy spread of about 130eV. If all these ions are allowed to pass through the magnet they would be dispersed both in energy and mass. In order to avoid the chromatic aberration due to such an energy spread a double focussing system is used. It consists of a combination of an ESA which disperses ions in energy and a magnetic sector (MS) which disperses them in mass. Ions emanating from a single point with same mass but different energies are dispersed in energy by the ESA and are brought back to the same focus by the magnetic sector. The ESA consists of two concentric electrodes which are held at fixed potentials such that ions with energy $\sim$ 4.5keV are transmitted along the principal axis while other ions are dispersed on either side depending on their energies. This produces an image of the crossover along the radial direction of the ESA. The energy slit (ES2) placed after the ESA allows ions of only certain energy bandwidth to reach the magnetic sector. These ions are then mass analyzed in the magnetic sector which has a radius of curvature of 12.5cm. The exit slit (ES3), placed after the magnet, allows mass(es) of interest to enter the detection system. One of the important criteria for isotopic analysis is symmetric peak shape and this is achieved by using the deflector (D2) and stigmator (S1) which allow one to make the entrance slit image parallel to the exit slit. The entrance and exit slits can be suitably adjusted to achieve the desired mass resolution.

There are several options at the detection end. Since the instrument can transport image, one can use the projector lens system (PLS) to produce image of the sample surface or the image of the crossover on the flourescent screen (FS) which is coupled to the channel

plate (CP). This allows us to use this instrument as an ion microscope. However this arrangement is generally used by us only to tune the instrument for isotopic analysis. The electrostatic deflector (EP) placed after the projector lens deflects the ions to the ion counting system where one has the choice of either using the Faraday cup (FC) or the electron multiplier (EM).

An electron multiplier (Balzer SEV217) is used for all isotopic analysis in this study. It consists of 17 stages and a potential of $\sim$ 2750V is applied across it when it is fresh (however this potential needs to be increased as the electron multiplier ages with time). The most important parameters of the electron multiplier that need routine checking are the efficiency and the dead time. However, instead of measuring the dead time of the electron multiplier, we opt to obtain the effective dead time of the total counting system (EM, preamplifier, discriminator and counting electronics) by measuring isotopic ratios in standard samples; this is described in a later section in this chapter.

2.2 High Mass Resolution Isotopic Analysis

The basic approach used for high precision, high mass resolution isotopic analysis using the ion microprobe has been discussed by many workers (Hutcheon 1982, Huneke et al. 1983, McKeegan et al. 1985, Ireland 1985 and Fahey et al. 1987a). The primary criteria to be satisfied for such an analysis are:

(i) resolution of isobaric, hydride, oxide and other molecular interferences at the mass(es) of interest,

(ii) dynamic stability of the magnet, and other instrument parameters during analysis,

(iii) suitable dead time (< 30nsec) of the counting system that is stable over a period of a few weeks or more,

(iv) proper sample preparation to avoid charging of the sample surface,

(v) a stable primary ion beam to minimize secular variation in secondary ion intensity.

2.2.1 Interferences and Corrections

The secondary ions that are generated from the sample surface consist of both atomic and molecular species (primarily hydrides, oxides, dimers and trimers) which may be singly or multiply charged. In addition, neutral species and electrons are also emitted from the sample surface. Any one of the charged species with a mass to charge ratio similar to the mass(es) of interest can act as an interfering species.

In general, hydride and oxide interferences in the low mass region ($A \leq 60$) can be resolved with a mass resolving power ($M/\Delta M$) of few thousand (where ΔM is the width of the peak at 10% of the peak count rate at mass M). However, separation of true isobaric interference (e.g. ^{48}Ti and ^{48}Ca) require a much higher mass resolution of $\sim$ 10,000. We have been able to resolve interference that require mass resolving power of upto 10,000 quite routinely with our ion microprobe. Several cases of resolved interferences, accomplished at high mass resolution with peak shapes having excellent flat tops and steep shoulders, are shown in Fig. 2.5.

In certain cases it is not possible to resolve the isobaric interferences (e.g. ^{46}Ca and ^{46}Ti; ^{50}Ti and ^{50}V; ^{40}K and ^{40}Ca etc.) and one has to indirectly correct such interferences. Additionally, when the mass of interest has a very low count rate compared to its neighbouring mass one has to correct for interference from the tail of the neighbouring peak, known as the tail correction and also take into account possible contribution from the dynamic background of the counting system. It is therefore necessary to consider all these aspects for each isotopic system carefully to resolve and/or correct for possible interference(s).

2.2.2 Dynamic Stability of the Instrument

Isotopic analysis using the ion microprobe is generally done in the flat-top peak-jumping mode. In this mode, the magnetic field values for the masses of interest are preset and the

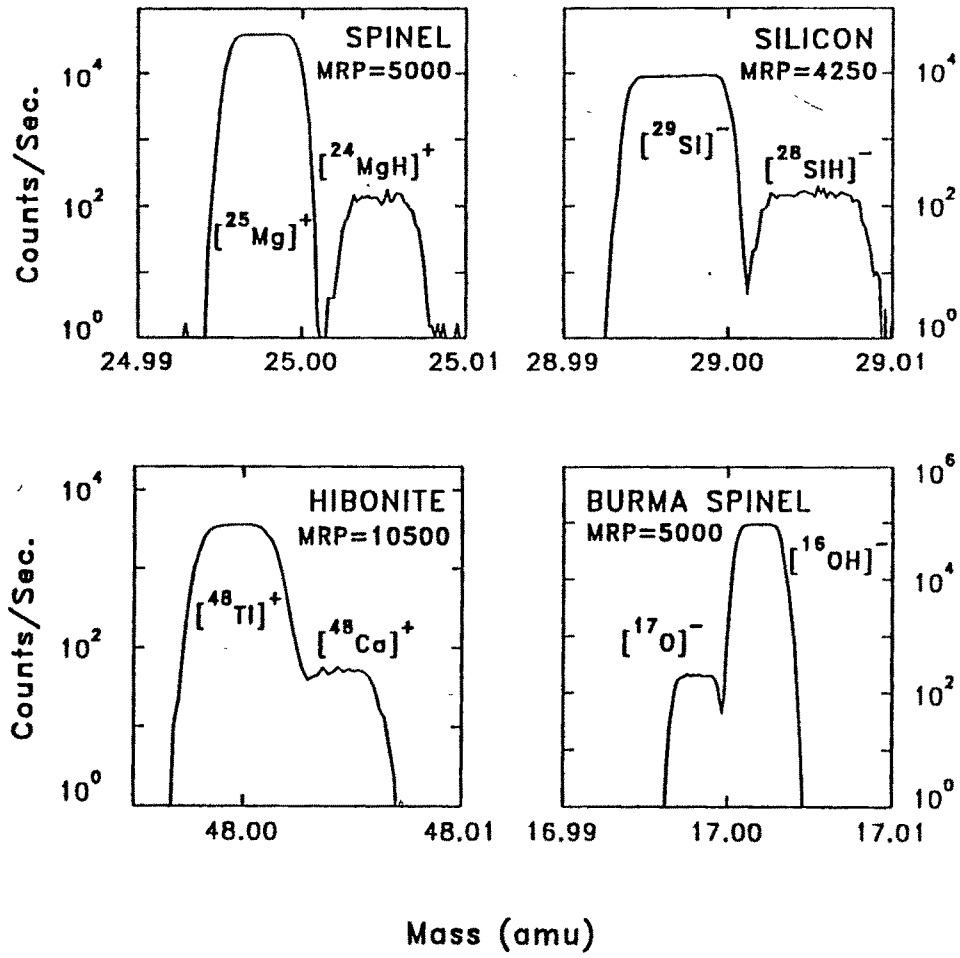

Figure 2.5: High mass resolution spectra at masses 25 (magnesium), 48 (calcium and titanium), 29 (silicon) and 17 (oxygen) showing well resolved hydride and true isobaric interferences. The mass resolving power (MRP = M/ΔM) and sample analyzed in each case are also indicated. Oxygen isotopic analysis was carried out using the Cs^+ primary ion beam in the negative secondary mode while the rest were analyzed as positive secondary ions with $^{16}O^-$ primary ion beam.

magnet is cycled through these masses with appropriate counting time for each mass. Five to eight such cycles constitute a block of data and each analysis typically comprises of data from 20 to 30 blocks. The magnetic field control of the Cameca Ims-4f has $\sim 2.6 \times 10^5$ fields bits that can be used for any one of the preselected mass ranges (1-20, 1-80, 1-280 amu). At high mass resolution ($M/\Delta M \geq 5000$), the flat top peak represents a small magnetic field interval ΔB, which is generally of the order of 10-15 field bits in the 1-80 mass range. Any instability in the instrument, especially in the magnet can alter the preset values for analyzed mass(es) beyond the flat top region leading to erroneous count rates. Therefore, several precautions have been taken to ensure a high degree of dynamic stability of the instrument; these include:

(i) extremely stable power supply for the ESA and other instrument sub-systems,

(ii) optimum temperature ($\sim 18 \pm 0.5$°C) for the magnet and ESA environments,

(iii) use of pre-adjusted voltages for the ESA,

(iv) a thick gold coating ($\sim$ 1000Å) of the sample to avoid progressive sample charging,

(v) an extremely stable counting system.

Since all these factors have a combined effect on the instrument performance, the dynamic stability of the instrument is measured in terms of the effective stability of the magnetic field in the peak-jumping mode of operation. Two mass regions (24-27) and (46-50) were investigated at a mass resolution of $\sim$ 5000 and count rates were measured at the peak centers of the chosen masses and at the left shoulder of the peaks where the count rate is approximately half that of the peak value. Since the count rate on the rising shoulder is extremely sensitive to changes in the effective magnetic field, the variation in the count rate at this position, relative to the peak center, provides an estimate of the fluctuation ($\Delta M/M$) in the mass which in turn can be related to the fluctuation ($\Delta B/B$) in the magnetic field. The value of $\Delta B/B$ provides a measure of the effective stability of the magnet (and hence the instrument) in the dynamic (peak-jumping) mode of operation.

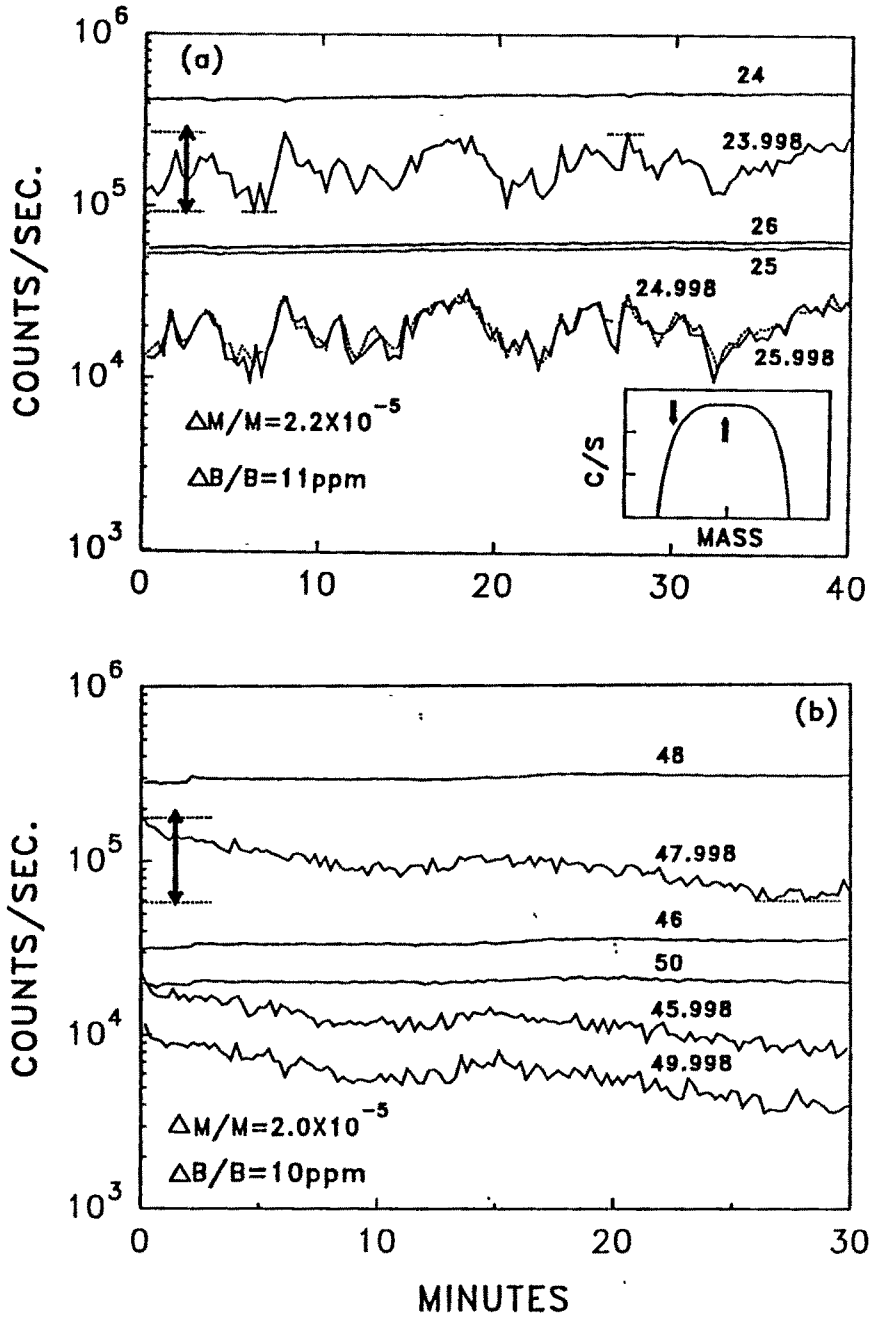

Figure 2.6: Count rates at the peak center (integer masses) and to the left of the peak center (non-integer masses) plotted as a function of time (see inset for approximate positions at which count rates are monitored). Two mass ranges: 24-26 (fig.a) and 46-50 (fig.b) are investigated in the dynamic (peak-jumping) mode of analysis. The values of $\Delta M/M$ and $\Delta B/B$ obtained from the maximum variation in count rate at the peak edge (marked by the vertical arrow) are shown in both the figures.

The results of these experiments are shown in Fig. 2.6. The "effective" value of $\Delta M/M$ is $\sim 2 \times 10^{-5}$ which translates into an effective stability of the magnetic field of about $\sim$ 10ppm for duration ranging from 30-40 minutes. In terms of magnetic field bits, e.g. at mass 24 this corresponds to about 3 field bits which is much less than the width of the flat top peak (about 15 field bits). Although the dynamic stability of our instrument is extremely good, the magnetic field values for the analyzed masses are automatically recalibrated during actual analysis after each block of data acquisition which generally takes $\leq$ 10 minutes. The shift in magnetic field during such recalibration is 1 to 2 field bits; this ensures that isotopic analyses do not suffer from temporal drift in the magnetic field and associated uncertainties.

2.2.3 Stability of the Counting System

The pulse counting system is used for all isotopic analyses carried out in this study. The stability of the counting system is extremely important for high precision measurement, and it is important to routinely monitor the efficiency, dead time and the background of the counting system. Tests are conducted to check the counting system comprising of the electron multiplier, preamplifier, discriminator and the counting electronics in an operative way by analyzing suitable terrestrial standards. The dead time is estimated by making measurements of isotopic composition of magnesium and titanium in terrestrial spinel and Ti-metal respectively at a mass resolution that can clearly resolve the hydride interference. The deviations in isotopic compositions from reference values are then attributed to the combined effect of isotopic mass fractionation and dead time of the counting system. Since the mass fractionation effect can be estimated by using appropriate fractionation law, one can determine the "effective" dead time of the counting system.

The results obtained from magnesium isotopic analysis in terrestrial spinel carried out in 1993 are shown in Fig. 2.7. The "effective" dead time of the counting system is (24$\pm$1)nsec for ^{24}Mg count rates ranging from $\sim$ 4X10^5 to 1.2X10^6 counts/sec(c/s). The dead time of the counting system generally remains stable over a time scale of several weeks and it is also a

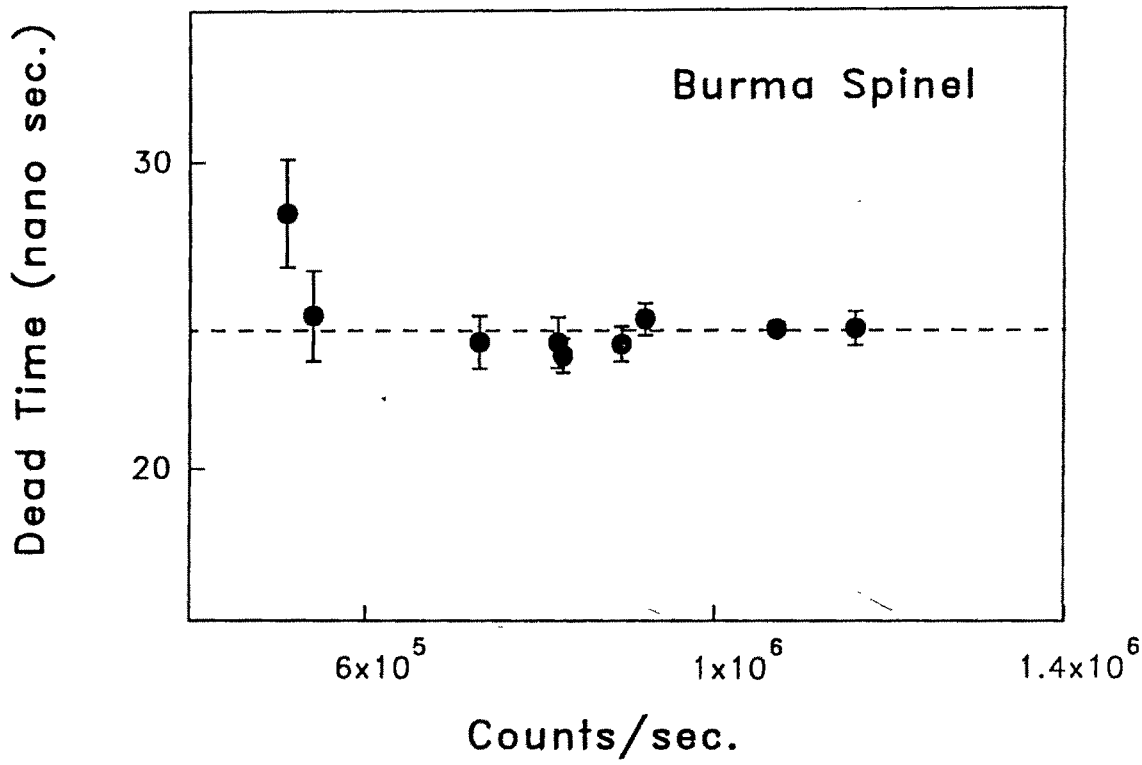

Figure 2.7: Dead time of the integrated pulse counting system as a function of count rate obtained from magnesium isotopic measurements in terrestrial spinel. Error bars are $2\sigma_m$.

function of the age of the electron multiplier. It may be noted that a similar exercise carried out in 1990 with a fresh electron multiplier gave a value of (19±1)nsec. During actual isotopic analysis the maximum count rate at any mass is generally kept below $2x10^5$(c/s) so that uncertainty in isotopic ratios due to uncertainty in the dead time is much below the limit set by counting statistics which is typically 1-2‰($2\sigma_m$).

The background of the counting system is ≤ 0.005(c/s) in the static mode (Fig. 2.8). In the dynamic (peak jumping) mode the background is monitored by obtaining count rates at a blank mass during isotopic analysis. The value obtained from several runs was ≤ 0.01 (c/s). Since the typical count rates during isotopic analysis are generally higher than this value by more than several orders of magnitude, the counting system background can be neglected during data analysis. The efficiency of the electron multiplier is generally $> 75\%$ and it is replaced when this value reaches $\sim 70\%$. The results obtained from the above parametric investigations of our ion microprobe show that it satisfies all the necessary conditions for carrying out high precision and high mass resolution isotopic analysis.

2.3 Isotopic Analysis of Terrestrial Standards

This section summarizes the results of measurements of isotopic composition of Mg, Ca and K in appropriate terrestrial standards. These analyses are a prerequisite for isotopic analysis of meteoritic phases, the primary aim of this work. Additionally, a set of isotopically doped anorthositic glasses were also analyzed to establish the precision and reproducibility that can be obtained during Mg isotopic analysis. These glasses have been used as internal standards by two other ion microprobe laboratories (Armstrong et al. 1982, McKeegan et al. 1985).

2.3.1 Mass Fractionation

The measured isotopic ratios of an element (e.g. Mg) in a standard can deviate from the reference isotopic ratios because of instrumental and intrinsic isotopic mass fractionation.

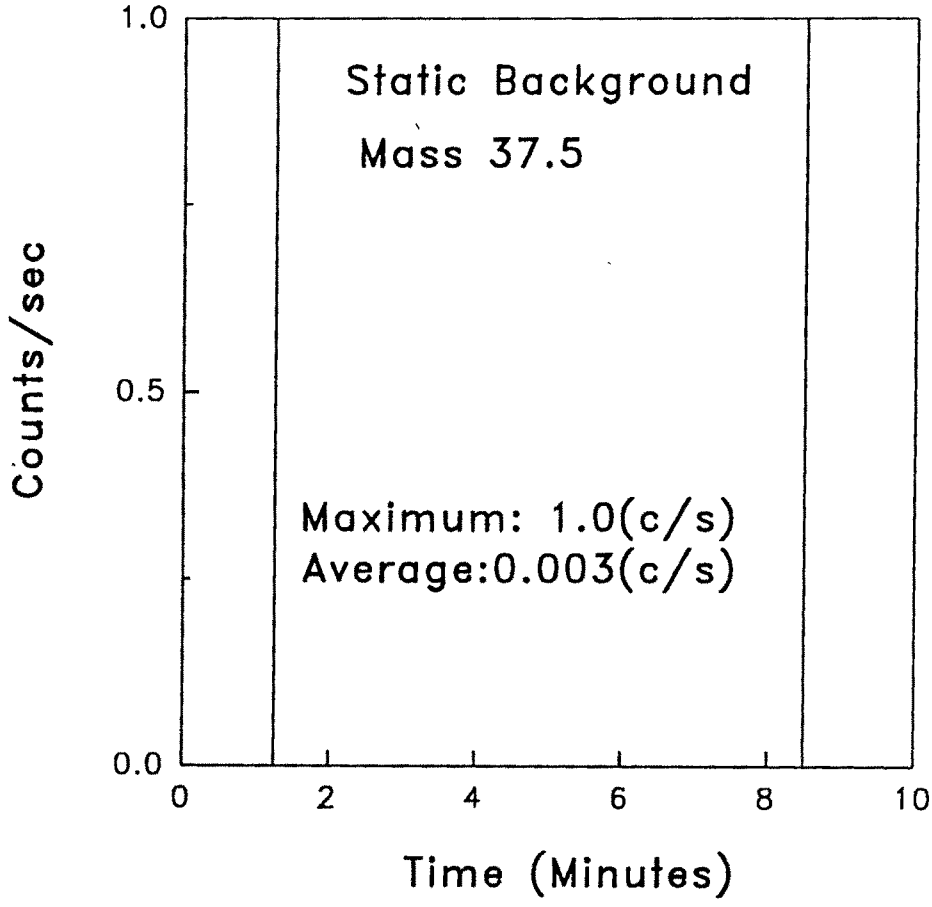

Figure 2.8: The static background of the pulse counting system at a dummy mass 37.5 over a period of ten minutes.

The process of generation, transmission and detection of secondary ions in an ion microprobe lead to instrumental mass fractionation. In addition, the sample itself could have undergone a variety of physico-chemical processes during its formation which could have altered the isotopic composition and this is referred to as the intrinsic mass fractionation or sample mass fractionation.

During the generation of secondary ions by the sputtering process, the lighter isotopes are in general preferentially sputtered compared to the heavier isotopes. Initially, the flux of lighter isotopes is strongly enriched, which decreases with time and finally a steady value is attained (Gnaser and Hutcheon 1987). The enrichment of lighter isotopes in secondary ions is strongly dependent on the sample matrix i.e. the nature of chemical bonding between the constituent atoms of the sample. Since all the ions have the same nominal energy of 4.5keV during transmission, the lighter isotopes with higher velocity are again fractionated preferentially compared to the heavier isotopes. During detection, by the electron multiplier, fractionation favours the lighter isotopes although the effect is very small, $\leq$ 1‰/amu (Zinner et al. 1986a). It is difficult to decouple the individual effects, and in general the total instrumental mass fractionation is estimated during analysis.

In case of terrestrial sample, the intrinsic fractionation is expected to be extremely small, and thus the measured fractionation in them can be attributed to instrumental mass fractionation. Further, the instrument mass fractionation for a given phase remains nearly the same as long as there are no changes in the ion microprobe tuning/operational conditions.

If we consider an element like Mg, which has three isotopes (24, 25 and 26), with reference isotopic ratios (normalized to ^{24}Mg) of ($^{25}Mg/^{24}Mg$) = 0.12663 and ($^{26}Mg/^{24}Mg$) = 0.13932 (Catanzaro et al. 1966); the deviations in the measured isotopic ratios from the reference values are generally expressed as:

$$\Delta^{25}Mg = \left[\frac{\left(\frac{^{25}Mg}{^{24}Mg}\right)_{meas.}}{\left(\frac{^{25}Mg}{^{24}Mg}\right)_{ref.}} - 1 \right] \times 1000 \text{ ‰}$$

$$\Delta^{26}Mg = \left[\frac{\left(\frac{^{26}Mg}{^{24}Mg}\right)_{meas.}}{\left(\frac{^{26}Mg}{^{24}Mg}\right)_{ref.}} - 1 \right] \times 1000 \text{ ‰} \qquad (2.1)$$

Since the total fractionation of any sample is a linear combination of instrumental and intrinsic mass fractionation, the intrinsic or sample mass fractionation of a meteoritic phase can be deduced by measuring isotopic mass fractionation of these phases and their terrestrial analogs under identical instrument operating conditions. If $[\Delta^{25}Mg]_{met}$ and $[\Delta^{25}Mg]_{std}$ represent the deviations for the meteoritic phase and its terrestrial analog, the intrinsic fractionation F(Mg) for the meteoritic phase is given as:

$$F(Mg) = \left[\Delta^{25}Mg\right]_{met} - \left[\Delta^{25}Mg\right]_{std} \text{ ‰/amu} \qquad (2.2)$$

In addition to intrinsic mass fractionation, the measured isotopic ratios in the meteoritic phases may differ from the reference values due to the presence of nuclear effect that can produce the isotope under consideration. Such an affect could be nucleogenic or radiogenic in origin and its presence can be ascertained when more than two isotopes of an element can be analyzed (e.g. Mg). One should however be able to choose at least two isotopes that are independent of the nuclear effect. The measured ratio of this pair of isotopes can be used to obtain the magnitude of isotopic mass fractionation. This will then allow one to infer the magnitude of fractionation effect for the other isotopes using suitable mass fractionation law. If any residual effect is present in the other isotopes, after due correction is made for the fractionation effect, it can be attributed to nuclear effect. The two relations generally used to describe isotopic mass fractionation are:

i) Exponential law:

$$\frac{R_m^{ij}}{R_r^{ij}} = \left(\frac{M^i}{M^j}\right)^p \tag{2.3}$$

ii) Power law:

$$R_m^{ij} = R_r^{ij}(1+\alpha)^{m_{ij}} \tag{2.4}$$

where R_m^{ij} and R_r^{ij} are the measured and reference isotopic ratios of the isotope i with respect to isotope j, M^i and M^j are the masses of the two isotopes, α and p are the fractionation parameters which are to be determined, and m_{ij} is equal to the difference in the masses of the two isotopes. When the degree of fractionation is small and mass difference m_{ij} is also small, one can use a linear approximation to these laws and they can be replaced by the linear law :

$$R_m^{ij} = R_r^{ij}[1+\alpha m_{ij}] \tag{2.5}$$

In the case of magnesium the isotopes 24 and 25 are used as the reference pair (free from nuclear effect) and one can use the linear law to show that the fractionation corrected residual, if any, in ^{26}Mg is given by :

$$\delta^{26}Mg = \left[\Delta^{26}Mg\right] - 2\cdot\left[\Delta^{25}Mg\right] \tag{2.6}$$

A non-zero value of $\delta^{26}Mg$ can be attributed to the presence of nuclear effect. In the case of Ca or Ti isotopes where the isotopic masses spread over a large range (40-48), (46-50) one cannot resort to linear approximation and it is necessary to use the exponential law to correct for fractionation and to infer the presence of nuclear isotopic effect (Fahey et al. 1987a).

2.3.2 Mg Isotopic Analysis

A set of terrestrial analogs of meteoritic phases were studied to determine instrumental isotopic mass fractionation ($\Delta^{25}Mg$) and $\delta^{26}Mg$ values. In terrestrial phases $\delta^{26}Mg$ is expected to be zero since no nuclear effects can be present in such samples.

The Mg isotopic analysis of the terrestrial standards were carried out at mass resolution ($M/\Delta M \sim 4000$) which is sufficient to resolve the major interferences from $^{48}Ca^{++}$, $^{48}Ti^{++}$, NaH^+ and MgH^+ at the masses of interest. The results of Mg isotopic analyses are shown in Table 2.1. The $\Delta^{25}Mg$ values for the different mineral phases represent the instrumental isotopic mass fractionation. The difference in these values for the various mineral phases is expected because of the differences in chemical bonding of Mg in them. Since extensive studies of Mg isotopic fractionation were planned on meteoritic phases it is important to establish that there is no significant temporal variation in instrument mass fractionation for magnesium isotopes ($\Delta^{25}Mg$) for a given phase under similar instrument tuning and operating conditions. We have measured $\Delta^{25}Mg$ in terrestrial spinel (Burma Spinel) at different time intervals over a 24 hour period. The results obtained in the study are shown in Fig. 2.9. All the values cluster within $1‰(2\sigma_m)$ of the mean value of 11.7‰, indicating excellent reproducibility of the magnitude of instrumental isotopic mass fractionation under a given instrument operating condition.

The $\delta^{26}Mg$ in the analyzed phases is indistinguishable from zero within the limit of our experiment uncertainties. The investigation of the possible presence of non-linear excess of ^{26}Mg in meteorite phases also requires the measurement of their Al/Mg ratio. Since the secondary ion yield can be different for different elements and is also dependent on the chemical composition of the sample, the relative yield for different elements has to be determined by using appropriate terrestrial standards of known composition. For example sensitivity factor λ for the Al-Mg system is defined as:

$$\left(\frac{^{27}Al}{^{24}Mg}\right)_{EP} = \left(\frac{^{27}Al^+}{^{24}Mg^+}\right)_{IP} \cdot \lambda \qquad (2.7)$$

Table 2.1: Mg Isotopic Data for Terrestrial Standards[‡]

Sample	N[†]	$^{27}Al/^{24}Mg$ $\pm 2\sigma_m$	$\Delta^{25}Mg$ $\pm 2\sigma_m$	$\delta^{26}Mg$ $\pm 2\sigma_m$
Burma Spinel*	4	2.59 ± 0.01	-11.62 ± 0.59	-2.04 ± 1.14
Spinel[@]	5	2.60 ± 0.02	-12.41 ± 0.66	-1.67 ± 1.28
Melilite[@]	6	1.32 ± 0.01	-7.81 ± 0.48	-0.60 ± 0.88
Madagascar Hibonite[#]	4	30.8 ± 1.50	-5.80 ± 0.84	1.25 ± 1.73
Lake County Plagioclase*	2	215.76 ± 8.10	-6.28 ± 1.90	0.72 ± 3.64

[‡]$\Delta^{25}Mg$ and $\delta^{26}Mg$ values are in permil
[†]Number of repeat measurements
[@]Vernadsky Institute, Moscow
[#]H. Curien et al. (1956)
*National Mueseum of Natural History, Smithsonian Institution, Washington, D.C.

Table 2.2: Mg-Al Sensitivity Factors

Mineral	λ
Melilite	1.04
Burma Spinel	1.40
Madagascar Hibonite	1.30
Lake County Plagioclase	1.24
Angra Dos ries Pyroxene	1.31

where EP and IP refer to electron probe and ion microprobe data respectively. The values for λ obtained by us for different minerals are given in Table 2.2.

To check the ability of our instrument to precisely measure non-linear excess in Mg isotopic composition, we have analyzed a set of anorthositic glasses doped with known amounts of ^{25}Mg. The Mg concentrations of these glasses are 200 and 1000 ppm. The results obtained by us are given in Table 2.3 and they are in very good agreement with the results obtained by two other ion microprobe laboratories as well as the gravimetric value. A small

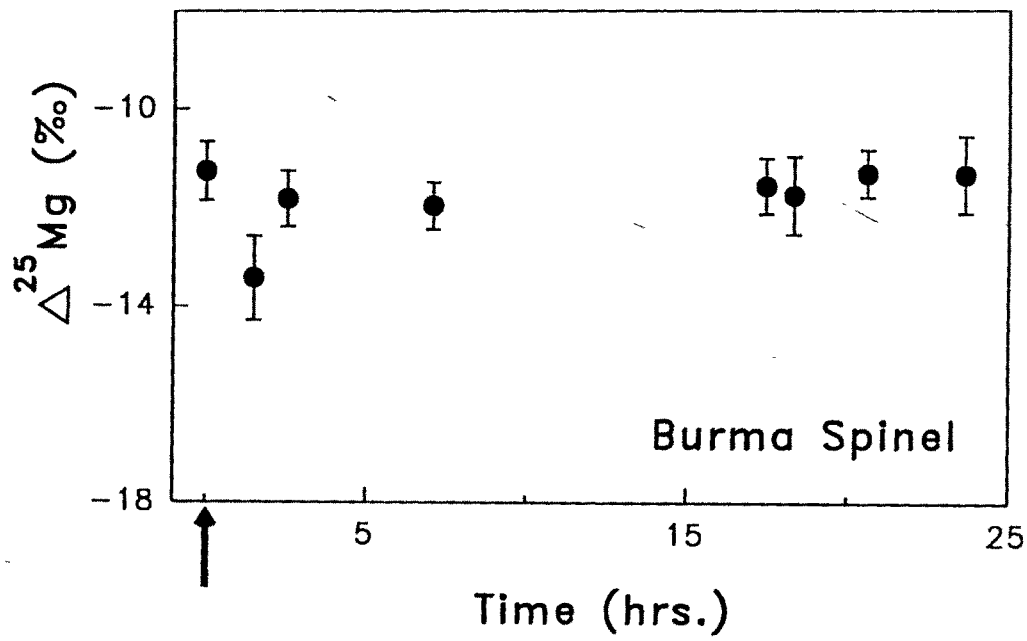

Figure 2.9: Magnesium isotopic mass fractionation in terrestrial spinel obtained from repeated analysis during a 24 hour run period. The arrow marks the start of the run. Error bars are two $2\sigma_m$.

difference can be seen in the case of the sample AN-MG-4, where the gravimetric value is lower than the ion microprobe data; this may probably reflect sample inhomogeneity. These results demonstrate our ability to measure non-linear excess in Mg isotope with a precision of 2‰($2\sigma_m$) even when the concentration of Mg is as low as 200ppm.

Table 2.3: Mg Composition of Isotopically Spiked Samples

Sample	Mg	δ^{25}Mg* ($\pm 2\sigma_m$) ‰			
Anorthositic Glass	ppm	Grav**	PRL	Panurge†	WU‡
AN-MG-1	292	0.0	0.3 ± 2.7	3.3 ± 3.4	1.9 ± 1.6
AN-MG-2	292	29.2	28.8 ± 1.9	31.4 ± 5.4	29.5 ± 1.6
AN-MG-3	292	101.7	100.8 ± 2.8	101.2 ± 4.7	99.2 ± 1.6
AN-MG-4	292	318.0	307.2 ± 2.5	310.0 ± 3.7	315.8 ± 1.7
AN-MG-5	1000	0.0	0.7 ± 1.8	2.2 ± 2.9	0.7 ± 2.2
AN-MG-6	1000	9.4	9.8 ± 1.7	9.1 ± 2.3	9.2 ± 1.5
AN-MG-7	1000	28.9	29.7 ± 2.7	29.6 ± 4.8	30.4 ± 1.9
AN-MG-8	1000	97.9	96.9 ± 2.2	96.7 ± 2.1	97.5 ± 1.9

*$\delta^{25}Mg = \Delta^{25}Mg - 0.5 \cdot \Delta^{26}Mg$

**Gravimetric Measurement

†Panurge (IMS-3F at Caltech): J. T. Armstrong et al. (1982)

‡WU (IMS-3F at Washington Univ.): K. D. McKeegan et al. (1985)

2.3.3 K-Ca Isotopic Analysis

One of the investigations conducted in this work was potassium isotopic studies of suitable meteoritic phases with high Ca/K to look for possible ^{41}K excess due to the decay of short-lived radionuclide ^{41}Ca ($\tau \sim 0.15Ma$). In order to check our ability to carry out such studies suitable terrestrial standards were analyzed for their K isotopic composition. In this section we summarize the procedures and precautions used in these measurements.

Studies of K-Ca isotopic system involves the determination of the sensitivity factors for K and Ca in suitable terrestrial analogs of meteoritic phases and accurate measurement of ($^{41}K/^{39}K$) since the abundance of ^{41}K is extremely small. Although K has three isotopes (39, 40 and 41), it is not possible to resolve ^{40}K from ^{40}Ca when Ca is present. Thus for all practical purpose K can be considered as a two isotope system in the present case.

K-Ca isotopic studies of terrestrial phases with high Ca/K were carried out at a mass resolution of ~ 5000 (Fig. 2.10), which is sufficient to resolve the major interference of ^{40}CaH at mass ^{41}K. However, the interference of $[^{40}Ca^{42}Ca]^{++}$ cannot be resolved at this mass resolution, and was corrected indirectly. The magnitude of the other unresolved doubly charged interference $[^{26}Mg^{56}Fe]^{++}$ is much smaller due to extremely low content of Fe in the Ca-rich phases and can be neglected. Finally, as the count rate at mass ^{41}K is extremely small compared to ^{40}CaH, it is also necessary to check for possible scattering from the tail of the hydride peak. A check of the dynamic background of the counting system is also necessary when the count rate of ^{41}K is $\leq 1(c/s)$. The measured ($^{41}K/^{39}K$) can therefore be written as:

$$\left(\frac{^{41}K^+}{^{39}K^+}\right)_{meas.} = \left(\frac{^{41}K^+}{^{39}K^+}\right)_{true} + \frac{\left(^{40}Ca^{42}Ca\right)^{++}}{^{39}K^+} + \frac{\left(^{40}CaH\right)^{+}_{tail}}{^{39}K^+} + background \qquad (2.8)$$

Since it is not possible to directly measure $[^{40}Ca^{42}Ca]^{++}$ count rate, we correct for it indirectly by finding the magnitude of $[^{40}Ca^{43}Ca]^{++}$ signal at mass 41.5 and noting that :

$$\frac{\left(^{40}Ca^{43}Ca\right)^{++}}{^{43}Ca^+} = \frac{\left(^{40}Ca^{42}Ca\right)^{++}}{^{42}Ca^+} \qquad (2.9)$$

The $[^{40}Ca^{43}Ca]^{++}$ signal can be monitored at 41.5. Since this signal is extremely low in both terrestrial and meteoritic phases, they were measured independently by using high primary current and large integration time to achieve good counting statistics. The measured values for $[^{40}Ca^{43}Ca]^{++}/^{43}Ca^{+}$ in terrestrial and meteoritic pyroxenes and terrestrial pervoskite are shown in Fig. 2.11. The results clearly demonstrate our ability to reproduce this ratio in these two mineral phases and we can use this ratio with confidence for correction of $[^{40}Ca^{42}Ca]^{++}$ interference. For the correction of possible contribution to $^{41}K^{+}$ signal from the tail of the hydride peak, we note that the $^{40}CaH^{+}$ signal is generally comparable or at times smaller (by a factor of two) than the $^{43}Ca^{+}$ count rate. Therefore we measured the count rate at mass (^{43}Ca - ΔM) for making this correction; where ΔM is given by the relation:

$$\Delta M = \frac{43}{41} \cdot \left[^{40}CaH - ^{41}K\right] = 0.009amu \tag{2.10}$$

The contribution from the tail of $^{40}CaH^{+}$ to $^{41}K^{+}$ is estimated as:

$$^{40}CaH_{tail}(c/s) = \left(^{43}Ca - \Delta M\right)(c/s) \cdot \frac{^{40}CaH^{+}}{^{43}Ca^{+}} \tag{2.11}$$

The potassium isotopic analysis was carried out by cycling the magnet through the masses ^{39}K, ^{40}CaH, ^{42}Ca, (^{43}Ca - ΔM) and ^{43}Ca in the usual peak-jumping mode. The counting time for signals at mass 39(^{39}K) and 41(^{41}K) were typically 30 to 60 sec respectively. Each analyses consisted of 10-12 blocks of 5 cycles each, which lasted for a duration of 90 to 120 minutes.

Relative sensitivity factors for Ca and K were measured in terrestrial pyroxenes with widely differing Ca/K ratios. The results are shown in Table 2.4 and we obtain a yield factor of $\sim$3.2 favouring K over Ca. We have used this yield factor for the perovskite phases also. The results of potassium isotopic analyses of terrestrial minerals with Ca/K ratios varying over nine orders of magnitude is shown in Table 2.5. The $^{41}K/^{39}K$ value in all the cases is

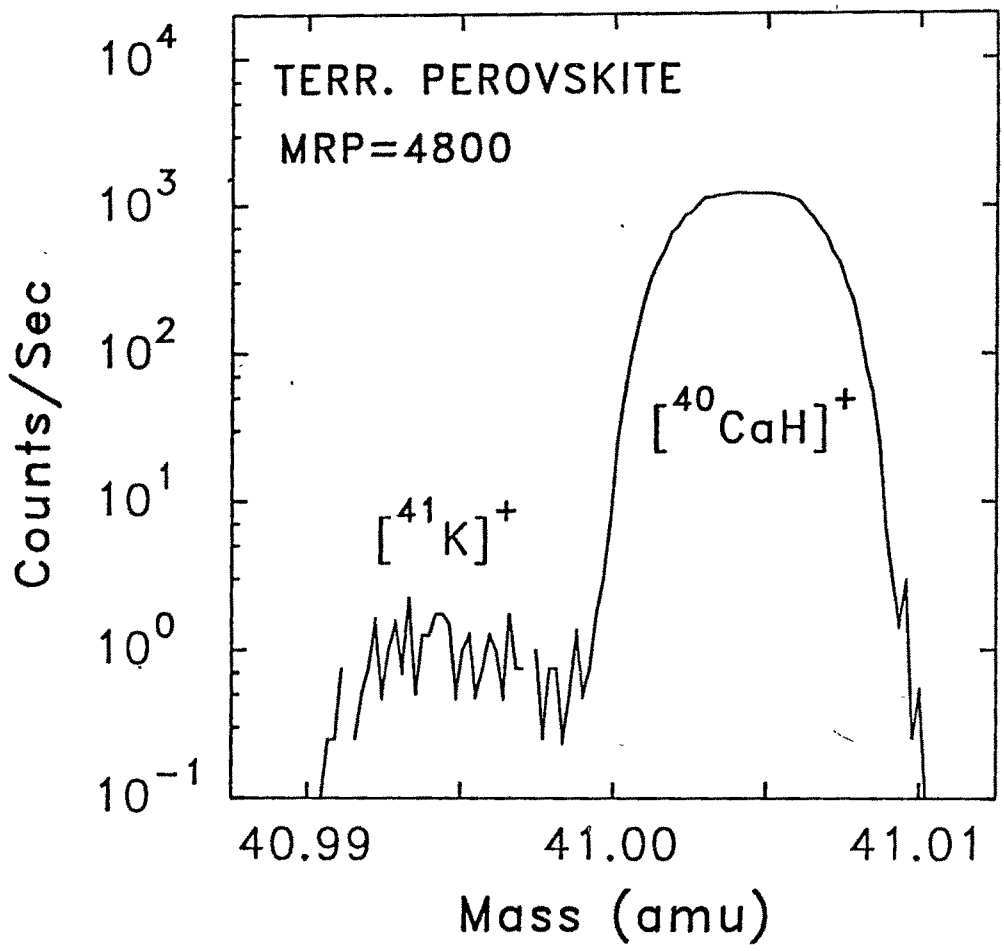

Figure 2.10: High mass resolution (mass resolving power: $M/\Delta M = 4800$) spectrum at mass 41 in terrestrial perovskite with $Ca/K > 10^6$ showing clearly resolved $^{41}K^+$ and $(^{40}CaH)^+$ peaks.

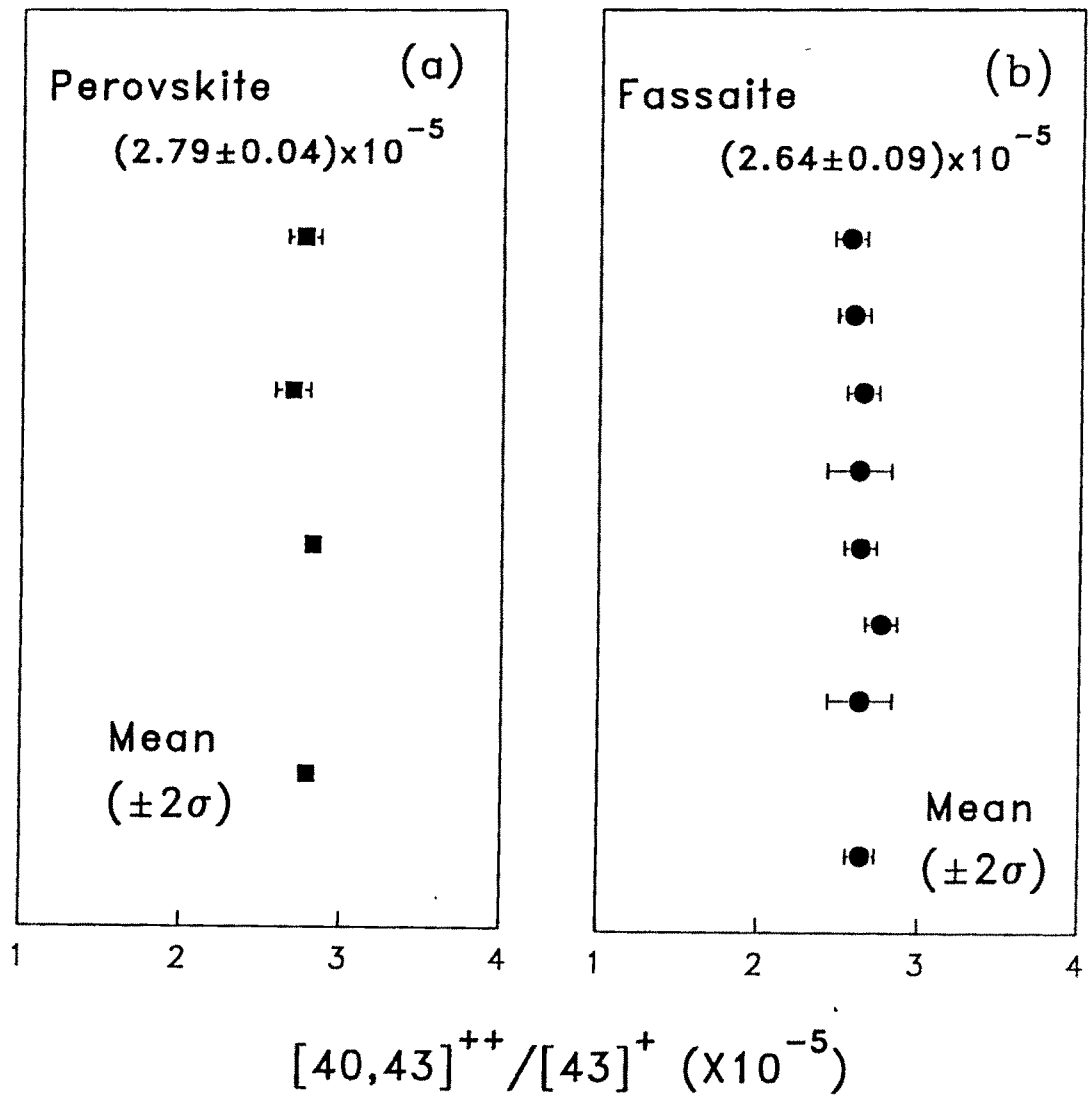

Figure 2.11: The values of $[^{40}Ca^{43}Ca]^{++}/^{43}Ca^{+}$ for individual runs in terrestrial perovskite [fig(a)] and meteoritic and terrestrial pyroxenes [fig(b)]. The mean values for the two phases are also indicated. Error bars are $2\sigma_m$

close to the reference value of 0.072, within the limits of experimental uncertainties. These results also suggest that the magnitude of intrinsic or instrumental mass fractionation in the case of potassium isotopes is extremely small.

Table 2.4: K-Ca Sensitivity Factors

Mineral	Ca/K	λ
Pyroxene 1	2.1×10^4	3.34 ± 0.10
(Ti-Px-1)	-	-
Pyroxene 2	3×10^6	3.08 ± 0.20
(CAI-Px-1)	-	-

All errors are $2\sigma_m$

Table 2.5: K Isotopic Analyses of Terrestrial Minerals

Sample	$^{40}Ca/^{39}K$	$^{41}K/^{39}K^{\ddagger}$ $\pm 2\sigma_m$
Microcline*	$\sim 10^{-3}$	0.07187 ± 0.0001
Anorthositic Glass ** (An-Mg-5)	8.6×10^3	0.07107 ± 0.0013
Pyroxene 1** (Ti-PX-1)	2.1×10^4	0.07301 ± 0.0012
Pyroxene 2** (CAI-PX-1)	3×10^6	0.06999 ± 0.0064
Perovskite@	$\sim 4 \times 10^6$	0.06475 ± 0.0091

* US National Museum Standard (USNM 143966).
**Samples prepared at Caltech (Courtesy I. Hutcheon).
@Sample obtained from Vernadsky Institute, Moscow.
‡Corrected for $(^{40}Ca^{42}Ca)^{++}$ interference.